



LAWRENCE
LIVERMORE
NATIONAL
LABORATORY

Final Task Report on NRF Measurements of Photon Scattering Resonances in Plutonium at the High Voltage Research Laboratory of MIT

Micah S Johnson, Dennis P McNabb, Eric B
Norman

February 27, 2007

Disclaimer

This document was prepared as an account of work sponsored by an agency of the United States Government. Neither the United States Government nor the University of California nor any of their employees, makes any warranty, express or implied, or assumes any legal liability or responsibility for the accuracy, completeness, or usefulness of any information, apparatus, product, or process disclosed, or represents that its use would not infringe privately owned rights. Reference herein to any specific commercial product, process, or service by trade name, trademark, manufacturer, or otherwise, does not necessarily constitute or imply its endorsement, recommendation, or favoring by the United States Government or the University of California. The views and opinions of authors expressed herein do not necessarily state or reflect those of the United States Government or the University of California, and shall not be used for advertising or product endorsement purposes.

This work was performed under the auspices of the U.S. Department of Energy by University of California, Lawrence Livermore National Laboratory under Contract W-7405-Eng-48.

**Final Task Report on
NRF Measurements of Photon Scattering Resonances in
Plutonium at the High Voltage Research Laboratory of MIT
Micah S. Johnson, Dennis P. McNabb, Eric B. Norman
January 27, 2007**

Measurements of nuclear resonance fluorescence (NRF) states in ^{239}Pu were conducted using the (γ, γ') reaction with Bremsstrahlung photons. The cross-sections of NRF states in ^{239}Pu were determined by taking the ratio of transition intensities in ^{239}Pu to the measured intensity of the 2212-keV transition of ^{27}Al .

The bremsstrahlung experiments were conducted at the 3-MV Van de Graaff electron accelerator at the High Voltage Research Laboratory (HVRL) at the Massachusetts Institute of Technology (MIT). Bremsstrahlung photons were produced by impinging an electron beam onto a "radiator" with 102- μm Au backed by 1-cm Cu (used for cooling and electron cleanup). The radiator was electrically isolated and the average current was recorded for analysis. The bremsstrahlung photons then pass through a 20-cm long collimator with a 2.5° half-angle, conic opening. The photon beam was aligned by steering the electron beam on the radiator and observing the tune of the beam with an x-ray imager downstream of the target.

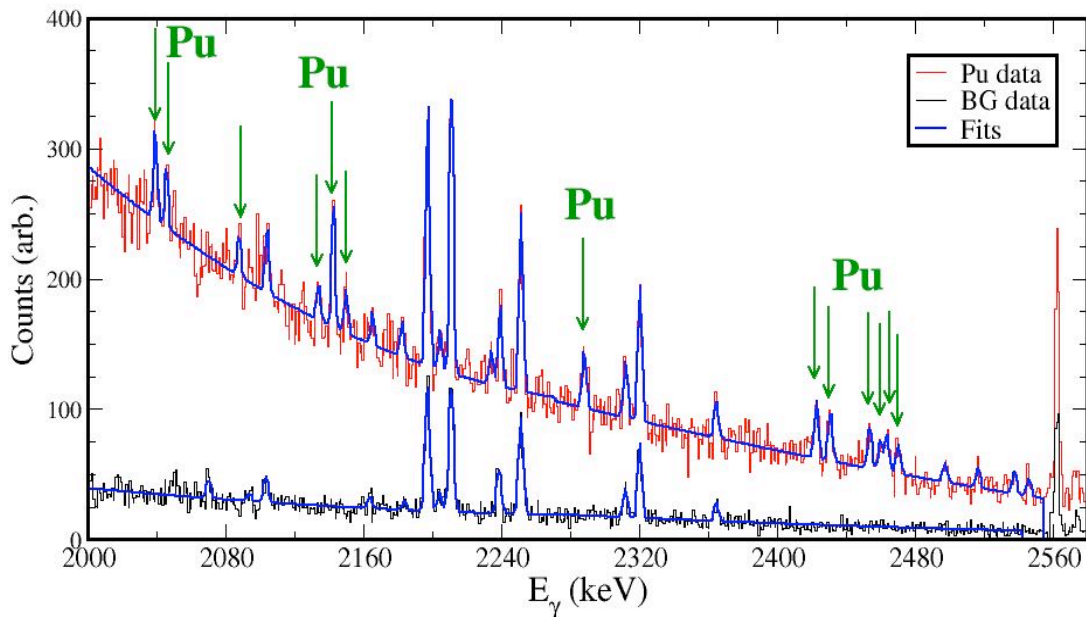
There were 2 targets for the Pu runs. Each target was a 1.5-cm diameter disk of ≈ 4 g of Pu enriched to 93% ^{239}Pu that was encapsulated in ≈ 25 -g Nitronic-40 holder with a 1-mil stainless steel window. The manganese of the Nitronic-40 (and other elements) did produce some contamination but also served as an internal energy calibration that will be discussed later. The outer diameter of the Nitronic-40 holder was approximately 2.5 cm. For normalization we placed a thin disk of Al (approximately 1.2 mm thick and 1.6-cm in diameter (similar to Pu diameter of 1.5 cm)) on the window of the Pu holder. We used two different target configurations during the Pu measurements. One, we used a single target at the central maximum of the bremsstrahlung beam. Second, we used two Pu targets side-by-side separated by approximately 1 cm and centered on the flux. Runs with the additional target increased our statistics by a factor of 2. The flux over this range was estimated with MCNP to be flat and was consistent with the online x-ray images.

Scattered γ -rays were measured with two HPGe detectors at 120° with respect to the beam direction in the lab frame. Both detectors were encased in thick Pb shielding to reduce background from room scatter. The openings to the detectors were covered with Pb absorbers of various thicknesses (e.g. 1/4",

1/2", 3/4", and 1") to reduce dead time at various end-point energies. The data rate for a 1" absorber at an end-point energy of 2.8 MeV was about 600 Hz for each detector and a dead time rate of 1-2%. With 3/4" absorbers the data rate increased to 5~kHz with a dead time of 17%. The data were collected in histogram mode with DSPEC electronic acquisition machines by ORTEC.

We explored the optimization of signal to background by taking measurements at end-point energies of 2.1 and 2.8 MeV. We found the 2.8-MeV endpoint to be best for two reasons. First, even at 2.8 MeV, the setup was found to be sensitive to strong NRF transitions down to 1.0 MeV. Second, the only states observed in the initial runs were at energies above 2 MeV.

The results for ^{239}Pu are shown in Fig. 1. The Pu histogram in Fig. 1 includes data from both target configurations and the dispersion is about 0.75-keV/channel. The background peaks, which can be seen in the lower (background) histogram of Fig. 1, are γ -ray transitions from NRF states in ^{55}Mn , ^{53}Cr , and ^{27}Al . The ^{55}Mn and ^{53}Cr are elements within the Nitronic-40 holder. The ^{27}Al is from the Al normalizer discussed in the previous section. States seen in the plutonium target data, but not in the blank Nitronic-40 background data, are associated with plutonium.



The 13 newly discovered Pu peaks in Fig. 1 were fitted with simple Gaussian line-shapes and the results are given in Tab. 1. To simplify the analysis, the results come only from runs done with the two-target configuration and an endpoint energy of 2.8 MeV. This data set had an integrated charge of 1.65 C on the radiator. Listed in Tab. 1 are the transition energy, confidence level, and cross-section strength for each new line assigned to plutonium. The energies were determined from energy calibrations of neighboring contaminate peaks for in ^{55}Mn , ^{53}Cr , and ^{27}Al . A total of 5 contaminate peak centroids were extracted and fit to a line. The largest contributions to the transition energy uncertainties were statistical.

Transition Energy (keV)	Confidence Level (%)	Integrated Cross-section (eV b)
2040.25(21)	100.	13(2)
2046.89(31)	93.3	9(2)
2089.14(35)	76.6	7(2)
2135.00(38)*	64.5	7(2)
2143.56(13) *	100.	22(3)
2150.98(31) *	96.4	9(2)
2289.02(26)	100.	15(3)
2423.48(23) **	100.	19(3)
2431.66(26) **	100.	16(3)
2454.37(26)	100.	16(3)
2460.46(38)	92.5	12(3)
2464.60(30)	97.9	15(3)
2471.07(34)	98.7	12(3)

The confidence levels in Tab. 1 are a convolution of two analyses. First, the probability that each peak is real and not a statistical fluctuation is given by

$$P_{peak} \approx (1 - e^{-\eta^2/2})^{N_f},$$

where η is the ratio of the measured peak area, A_{fit} , and its uncertainty, $\sigma_{A_{fit}}$ and N_f is the number of peak-like fluctuations one might expect in a given fit range.

Second, the probability that the measured peak is unique to the target data and not present in the background data was determined. Our method to estimate this probability utilized a fit to the background data, fixing the width and centroid characteristics of the peak extracted from the Pu target data. The probability that there is a peak in the background data of area x is given by

$$P(x, B_{fit}) \approx e^{-(x-B_{fit})^2/2\sigma_{B_{fit}}^2},$$

where B_{fit} and $\sigma_{B_{fit}}$ are the fitted area and uncertainty of the peak in the background data. Two possibilities were considered: either the background data is consistent with not having this peak (i.e. an area of zero counts) or the background data is consistent with a scaled peak area, $a_{fit} \equiv S A_{fit}$ where S is the ratio of integrated charge of the background run divided by the integrated charge of the target run. The fraction of the target peak area that is consistent with 0 counts is taken to be

$$O(B_{fit}, 0) \equiv \int_{-\infty}^{\infty} dx \cdot P(x, B_{fit}) \cdot P(x, 0),$$

where the uncertainty, σ_0 , is determined from the fluctuations in the background spectrum. The fraction of the target peak area that is consistent with a_{fit} of the background data is $O(B_{fit}, a_{fit})$. Effectively, $O(B_{fit}, a_{fit})$ determines whether or not the measured peak is part of the target holder.

In summary, the confidence level given in Tab. 1 that the peak is real and associated with the Pu target is defined as:

$$CL \equiv P_{peak} \cdot \frac{O(B_{fit}, 0)}{O(B_{fit}, 0) + O(B_{fit}, a_{fit})}$$

Two approaches were used to derive the integrated cross sections from the fitted peak areas. In both approaches, the fitted peak areas were corrected for attenuation of the incident flux and for attenuation of the resonantly scattered photons on their way back through the target holder and Al disk. The incoming attenuation correction included electronic and nuclear attenuation. The outgoing attenuation correction consisted of electronic attenuation only. In both cases the attenuation correction was performed assuming that scattering interaction took place in the middle of the plutonium foil. The nuclear attenuation coefficient was estimated using an approximate cross-section of 20 barns.

The integrated cross-sections listed in Tab. 1 for Pu were deduced by comparing the intensities of the Pu peaks to the 2212-keV transition of ^{27}Al and the known strength of that state, $T_{1/2} = 26.4(7)$ fs [ENSDF]. The integrated cross-sections for Pu and Al were then made into a ratio and the integrated cross-section for Pu was extracted. Steps were taken to account for the energy difference of the resonance energies in Pu to the 2212-keV level of ^{27}Al . First, a correction for an energy-dependent detection efficiency was calculated with GEANT4. Second, MCNP was used to correct for energy-dependence in the incident flux. The largest source of uncertainty in the integrated cross-sections was counting statistics.

To verify the accuracy of the ratio approach for Pu, we also determined the integrated cross-sections of the resonances listed in Table q via an absolute method. The integrated cross-section is given by $\int \sigma dE = A'_{\text{fit}} / \epsilon \Phi N$, where ϵ is the energy-dependent detection efficiency (intrinsic and geometric), Φ is the energy-dependent photon flux per unit energy from the bremsstrahlung source subtended by the target area, and N is the number of target atoms per unit area. A'_{fit} is the peak area, corrected for the attenuation. The measurements and simulation results were combined using the above expression for the integrated cross-section. The integrated cross-sections from this method are in agreement with those listed for in Table 1 from the ratio method to within 1 sigma.

The integrated cross sections in Tab. 1 do not include corrections for non-isotropic scattering. Angular distribution effects are expected to greatest if the transition is from a spin 3/2 to the 1/2 ground state in ^{239}Pu versus a 1/2 to 1/2 transition. Such a transition would cause an approximate 15% decrease in the cross-section strengths given in Tab. 1. (This was estimated using average angular distribution coefficients measured in $^{203,205}\text{Tl}$ for 3/2 to 1/2 transitions by Hausser *et al.* [Nucl. Phys. A314 161, (1979)]). The largest source of uncertainty in the cross-sections for Pu were from the uncertainties in the peak areas due to low statistics. The uncertainties in peak areas ranged from 15-40% .

Further evidence that the above transitions in Tab. 1 are indeed associated with ^{239}Pu comes from the energy difference between some of the centroids. The energy difference between the ground state and first excited state in ^{239}Pu is 7.861 keV [ENSDF]. Selection rules indicate that a state populated from the ground state can decay to either the ground state or first excited state. For example, the γ -ray pair highlighted in Table 1 by ** are separated by 8.2(4) keV, consistent with 7.861 keV. In this case, a proposed level at ~ 2.431 MeV is populated with an incident γ -photon and decays via one of two branches: direct 2131-keV γ -ray to the ground state and the intermediate γ -ray 2423(3)-keV to the 7.861-keV level. If this indeed true, then we are within reason to assign the integrated cross-section of the 2.431-MeV level a value of 35(4) eV b. Following through with this assessment, the branching ratio from the 2.431-MeV level is 45.6(7)% to the ground state. Two other candidates for branched decay can be found with the three states marked with an * in Table 1. We estimate that only part of the strength in the 2.143-MeV level is associated with a direct transition to the ground state from a resonance at 2.143 MeV. Our hypothesis is that the remainder of the strength is associated with a branch to the first excited state from a proposed level at ~ 2.151 MeV. The remainder of the decay strength from the 2.143-MeV level goes directly to the ground state via a 2151-keV transition. Unfortunately, the

energy difference between 2151 keV and 7.861 keV puts the intermediate γ -ray energy at the same energy (within uncertainties) as the 2.143-MeV proposed level.

In conclusion, 13 new transitions associated with NRF states in ^{239}Pu have been discovered. These resonances are between 2- and 2.5-MeV relative to the ground state in ^{239}Pu . The strengths of most these resonances are between 15 and 20 eV b. This approximately is the strength required for using the transmission detection method for NRF [Pruet *et al.* *J. Appl. Phys.* **99** 12310 (2006)] for six-sigma alarm confidence levels.

Future measurements on ^{239}Pu at higher photon energies are necessary to probe for NRF strengths at higher energies. Such resonances may be more advantageous to the NRF technique with FINDER if they are stronger or if the mean free path of these energetic photons is longer.